Anticorrosive Behavior and Porosity of Tricationic Phosphate and Zirconium Conversion Coating on Galvanized Steel

Camilo S. Velasquez, Egnalda P.S. Pimenta, and Vanessa F.C. Lins

This work evaluates the corrosion resistance of galvanized steel treated with tricationic phosphate and zirconium conversion coating after painting, by using electrochemical techniques, accelerated and field corrosion tests. A non-uniform and heterogeneous distribution of zirconium on the steel surface was observed due to preferential nucleation of the zirconium on the aluminum-rich sites on the surface of galvanized steel. The long-term anti-corrosion performance in a saline solution was better for the phosphate coating up to 120 days. The coating capacitance registered a higher increase for the zirconium coatings than the phosphate coatings up to 120 days of immersion. This result agrees with the higher porosity of zirconium coating in relation to the phosphate coating. After 3840 h of accelerated corrosion test, and after 1 year of accelerated field test, zirconium-treated samples showed an average scribe delamination length higher than the phosphate-treated samples.

1. Introduction

One of the most commonly used corrosion protection systems in the automotive and manufacturing industries is the use of metal coatings in conjunction with organic coatings (duplex systems). The properties of the combined coatings have a synergistic effect, increasing the corrosion resistance and extending the lifetime of the substrate (Ref 1, 2). However, despite the satisfactory performance offered by duplex systems in terms of corrosion resistance, conversion coatings are used as an intermediate layer before the application of organic coatings to promote adhesion on metal surfaces (Ref 3). These treatments provide a porous and a greater roughness surface than the untreated metal surface, increasing the anchoring between the metal and the painting (Ref 4).

Phosphate conversion coatings have been used for many years for this purpose, due to their operating time, wear resistance and adhesion properties. However, this kind of process presents several environmental limitations. The acid wastes from phosphate baths have a detrimental effect on water effluents leading to eutrophication processes; the phosphating sludges generated throughout the process are considered as hazardous material and potentially carcinogenic; and phosphating baths typically work between 30 and 99 °C, which means that it has a high energy consumption (Ref 3, 5).

In the last years, nanoceramic-based conversion coating has been studied as possible substitute of the phosphate treatment. One of the alternatives developed is zirconium conversion coatings, which have a low energy demand as they are produced at room temperature, generate less sludge and does not incorporate toxic elements that may endanger human health (Ref 6, 7).

According to Adhikari et al. (Ref 3), zirconium surface pretreatment, by immersion in hexafluorzirconium solutions (H_2ZrF_6), has shown corrosion resistance comparable to phosphated cold rolled steel. Similar results were obtained by Gusmano et al. (Ref 8) on zirconium-treated aluminum substrates by the sol–gel method. Verdure et al. (Ref 9) studied the mechanism of formation of hexafluorozirconic and hexafluorotitanic on magnesium alloy AM60, suggesting a preferential nucleation of the Zr and Ti on cathodic particles existing on the alloy surface. Similarly, Ghanbari et al. (Ref 10) reported that the precipitation of the Zr compounds occurred in the microcathode area of the mild steel surface, leading to the formation of intermittent and porous zirconium layer (uncovered areas).

Electrochemical impedance spectroscopy (EIS) is a powerful tool for the characterization of protective coatings, as well as for obtaining information about porosity, water uptake and barrier properties. Different authors have reported the importance of porosity in the anti-corrosion performance of coated materials (Ref 11, 12). However, quantitative evaluation of the porosity degree by electrochemical techniques is rarely reported in the literature.

In this paper, electrochemical impedance spectroscopy was used to evaluate the corrosion resistance and porosity of tricationic phosphated and zirconium-treated galvanized steel. Accelerated (GM 14872) and field (ISO 11474) tests were also used to study the effect of zirconium pretreatment on the corrosion resistance of painted samples. Morphological aspects of the treated samples were performed by scanning electron microscopy (SEM) and energy-dispersive spectroscopy (EDS).

Camilo S. Velasquez and **Vanessa F.C. Lins**, Chemical Engineering Department, Universidade Federal de Minas Gerais, Antonio Carlos Avenue 6627, Belo Horizonte 31270901, Brazil; **Egnalda P.S. Pimenta**, USIMINAS Industry, Ipatinga, Brazil. Contact e-mails: camisave@gmail.com egnalda.pimenta@usiminas.com, and vlins@deq.ufmg.br.

2. Methodology

2.1 Materials and Sample Preparation

Hot-dip galvanized steel panels without heat treatment and dimensions of 100 mm × 150 mm × 1 mm were obtained from the industrial line of a Brazilian steel industry. The composition of the substrate (mild steel) in wt.% was listed as the following: 0.0015% C, 0.14% Mn, 0.010% S, 0.014% P, 0.01% Si, 0.060% Ti, 0.020% Nb and 0.050% Al. The phosphated samples were cleaned with deionized water and degreased for 300 s with a 3 wt.% alkaline solution (Parco Cleaner 1522A/V) at 65 °C and rinsed with water at room temperature. The steel samples were then immerged in an aqueous solution of 6 gL^{-1} of a titanium-based refiner for 45 s at room temperature; the titanium containing a conditioning chemical promotes the formation of a fine-grained phosphate coating. A commercial solution of tricationic phosphate (Granodine 958R) was used for 191 s at 55 °C and then rinsed with running water for 60 s at room temperature. Finally, a solution of Parcolene 90A was used as passivant for 45 s at room temperature.

The steel samples were cleaned with deionized water and an alkaline solution. The zirconium conversion coating was applied by dipping in a conversion solution prepared from hexafluorozirconic acid (H_2ZrF_6) with 90 mg/L Zr (TecTalis 1800) at room temperature. The pH of the solution was adjusted to 4, and the immersion time was 90 s. After immersion, all the samples were rinsed with water at room temperature.

The surface-treated galvanized steel panels were painted with an epoxy primer by cathodic electrophoretic deposition for 24 s. Then, it was cured in the oven for 24 s at 165 °C. A polyester resin was applied as primer by spraying, and the cure was carried out at a temperature of 140 °C for 24 s. The base coat was sprayed with a polyester resin and a varnish of acrylic resin. Finally, the painted steel panels were cured in the oven for 30 s at 140 °C and cooled down to room temperature.

2.2 Surface Morphology

The morphology of the treated and untreated steel samples was studied using a Microscope FIB-Quanta FEG 3D FEI with an acceleration voltage of 5-15 kV. Energy-dispersive x-ray spectrum (EDS) was also used to provide elemental distribution mapping on the surface.

2.3 Electrochemical Measurements

Electrochemical impedance spectroscopy (EIS) was performed to compare the long-term anti-corrosion performance of tricationic phosphate and zirconium conversion coating after the application of painting system. EIS measurements were taken after different immersion periods of 80, 100 and 120 days in a 3.5 wt.% NaCl aqueous solution. EIS studies were carried out in the frequency range of 10 kHz-10 mHz with the acquisition of 10 points per decade and an amplitude of the perturbation of 10 mV. An Autoload PGSTAT 252 equipment was used with a three-electrode configuration to perform the electrochemical measurements. The working electrode was treated coated samples with exposed area of 1.3 cm^2, and saturated Ag/AgCl was used as the reference electrode and platinum foil as auxiliary electrode. All tests were conducted after open-circuit potential (OCP) stabilization for 60 min in a 3.5 wt.% NaCl solution.

2.4 Conversion Coating Porosity

The determination of the porosity becomes an important parameter for estimating the corrosion resistance (Ref 13, 14).

The coating porosity can be evaluated using Eq 1 (Ref 12).

$$P = \frac{R_p'}{R_p} \times 10^{-(\Delta E_{corr} / \beta_a)} \tag{Eq 1}$$

where P is the coating porosity, R_p' the polarization resistance of bare substrate, R_p the polarization resistance of coated substrate, ΔE_{corr} the corrosion potential difference between the bare substrate and the coated substrate, and β_a the anodic Tafel coefficient of bare substrate.

The values of R_p and R_p' were obtained by electrochemical impedance spectroscopy (EIS) after 60 min of immersion for stabilization of open-circuit potential in a 3.5 wt.% NaCl solution. The potential amplitude was 10 mV, and the scan range of frequency was from 100 kHz to 10 mHz with acquisition of 10 points per decade.

The anodic Tafel coefficient of bare substrate (β_a) was estimated by Tafel analysis using Nova 1.11 software. The polarization potential range was ± 250 mV with respect to the open-circuit potential (OCP), and a scan rate of 0.167 mV/s was applied. The electrochemical tests were performed by using an Autolab PGSTAT 252 equipment. The electrolyte was a 3.5 wt.% NaCl solution at room temperature.

2.5 Accelerated and Field Corrosion Tests

Before accelerated corrosion tests (GM 14872 standard) (Ref 15) and field tests with a saline solution spray (ISO 11474 standard) (Ref 16), the painted steel samples were scratched using a flat tool to achieve the base metal according to the ASTM D1654-08 standard (Ref 17). This artificial defect acted as an initiation point for the corrosion.

2.5.1 Cyclic Accelerated Corrosion Test GM 14872. Cyclic humidity testing was performed using the GM 14872 standard with a testing time of 3840 h, corresponding to 160 cycles of 24 h. Salt solutions (0.9% w/v NaCl, 0.1% w/v $CaCl_2$ and 0.075% w/v $NaHCO_3$) were sprayed directly on the test samples for 15 min. Samples remained in the wet chamber for 75 min at 25 ± 2 °C without salt spray. This procedure was repeated 4 times before the next step.

The coated samples were exposed in the chamber for 2 h at 25 ± 2 °C and relative humidity > 30%. The third stage consisted by 8-h exposure to a water fog humidity climate of 100% (relative humidity) at 49 ± 2 °C. The fourth stage consisted by 7 h in dry chamber with relative humidity less than 30% at 60 ± 2 °C. Samples were then exposed in the chamber at 25 ± 2 °C and relative humidity < 30%. Equipment used was Q-Fog of Q-Panel Company.

2.5.2 Accelerated Field Tests with a Saline Solution Spray. The atmospheric corrosion tests of the painted panels were carried out at a corrosion station located at an altitude of 247 m and 19°29′09″S latitude and 42°32′01″W longitude, in Brazil. This test was performed according to the ISO 11474 standard, with a spraying of an aqueous solution of 3% w/v NaCl twice a week.

The wet surface of this test period was 50% and the corrosiveness was of 2.6 kg Fe/m^2 year, well above that of the marine environment which was 0.6 kg Fe/m^2 year. The classification of the testing atmosphere was C5 according to the ISO 9223 standard, a very high aggressiveness.

3. Results and Discussion

3.1 Sample Characterization

Figure 1(a) shows the micrographs of the galvanized steel sample. The crystals of the zinc coating are of minimized shape and have morphology in form of dendrite arms. This is a characteristic of galvanized steels without heat treatment; a high nucleation rate during the cooling process tends to bring about the formation of small grains in the zinc matrix (Ref 18).

In this kind of galvanized steel, it is possible to verify the presence of aluminum in the zinc layer. Aluminum is intentionally added in the steel production process with the aim of slowing down the zinc–iron reaction rate, thus forming a layer of pure zinc, and in this case, iron–aluminum and not iron–zinc intermetallic compounds are produced in equilibrium with the liquid. Aluminum additions of 0.135 wt.% at 723 K are sufficient to precipitate an iron–aluminum phase on the steel surface (Ref 19). The most common industrial hot-dip zinc coatings used in Brazil are GI (Zn-0.2 wt.% Al), studied in this work, galvalume (55 wt.% Al, 43.5 wt.% Zn, 1.5 wt.% Si) and galvanneal obtained by annealing at temperatures from 490 to 540 °C (Ref 20). The EDS mapping (Fig. 2) confirmed the significant presence of aluminum and oxygen as oxides in the surface layer; this segregation of aluminum may act as an impurity or intermetallic compound that compromises the continuity and performance of the metallic coating.

As seen in the micrographs of Fig. 1(c), the zirconium-treated surface appears formed of small round particles. The nature of the deposited layer is not continuous and did not cover the entire surface, and this means that oxidizing agents can easily corrode the substrate as they penetrate through the defects of the coating.

The EDS mapping results (Fig. 3) confirmed the absence of zirconium in some regions of the treated steel surface. The red regions on the EDS mapping represent discrete areas of zirconium deposit (Fig. 3), while the blue regions are uncovered surface.

According to Zr, Zn and Al EDS maps (Fig. 4), zirconium appears deposited along the treated surface on the aluminum-rich phases (marked areas). These results indicate that the surface coverage of the conversion coating is non-uniform. Different authors have reported the preferential deposition of zirconium over cathodic intermetallic, suggesting that microstructure of substrate plays a key role in the mechanism of deposition of zirconium coating (Ref 9, 21, 22).

3.2 Corrosion Resistance of Painted Samples

Electrochemical impedance spectroscopy (EIS) has been performed after immersing test for various times in 3.5 wt.% NaCl solution, to evaluate the long-term corrosion behavior of conversion coating with painting.

During the first 80-day immersion, the Nyquist plots (Fig. 5a) show one capacitive semicircle in the high frequency range of spectra for the phosphate layer and zirconium-based layer. Impedance modulus of 10^7 Ω cm^2 (Fig. 5b) was obtained for the two systems under study (phosphate and zirconium treatment). The existence of this semicircle in the EIS spectra indicates that the degradation of the paint has begun. Paint coating degradation involves the penetration of ionic species, the changes in the coating adherence and the development of pores or microdefects in the coating layer (Ref 23, 24).

Bode plot (phase angle versus frequency) after 100 days of immersion in 3.5 wt.% NaCl solution is shown in Fig. 6(c), and a new time constant appeared in the impedance diagram. This means that the electrolyte has passed through the organic coating, via short-circuit paths, reaching the substrate and initiating the under-paint corrosion. Analyzing Bode plot of Fig. 6(c), it can also be seen that the zirconium-based conversion coating has a phase angle close to $-80°$ at high frequency (from 10 to 10,000 Hz) which is reported as the region where the capacitive response of the organic coating is observed. The phase angle response indicates a faster loss of barrier properties of zirconium-treated samples than phosphate-treated samples (phase angle of $-90°$). The impedance modulus for both systems (Fig. 6b) decreased one order of magnitude (10^6 Ω cm^2) when compared with phosphated and zirconium-treated samples after 80 days of immersion in NaCl solution.

After 120 days of immersion in NaCl solution, the impedance spectrum exhibited two distinctive semicircles (Fig. 7a). The first semicircle, at high frequencies, is associated with the interface parameters such as organic coating contribution, and the second semicircle, at low frequency, refers to the charge transfer resistance at the coating–substrate interface. The Nyquist plot shown in Fig. 7(a) presents a relevant loss of
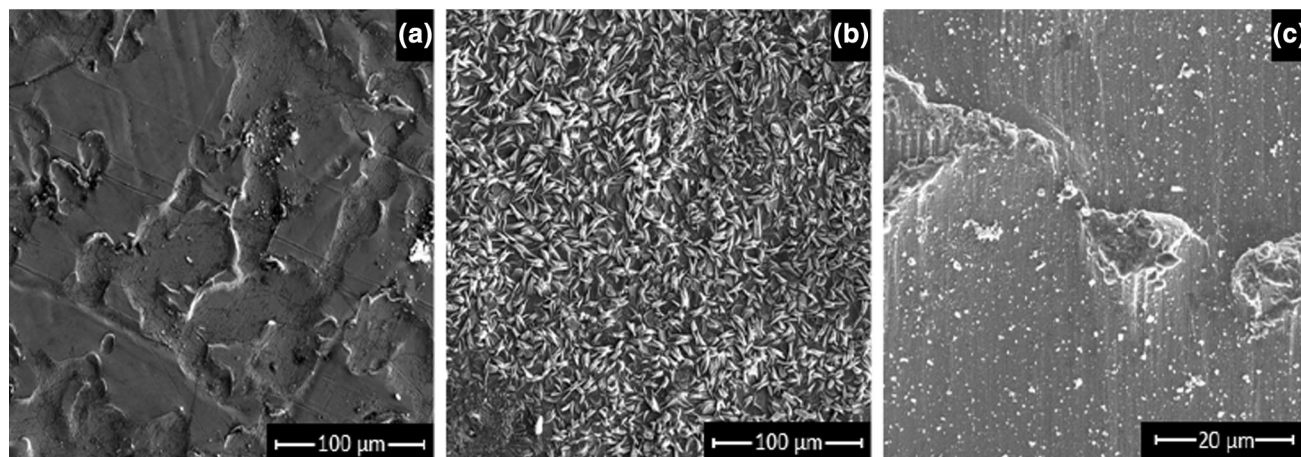
Fig. 1 Surface morphology of: (a) bare galvanized steel, (b) phosphated steel and (c) zirconium-treated steel
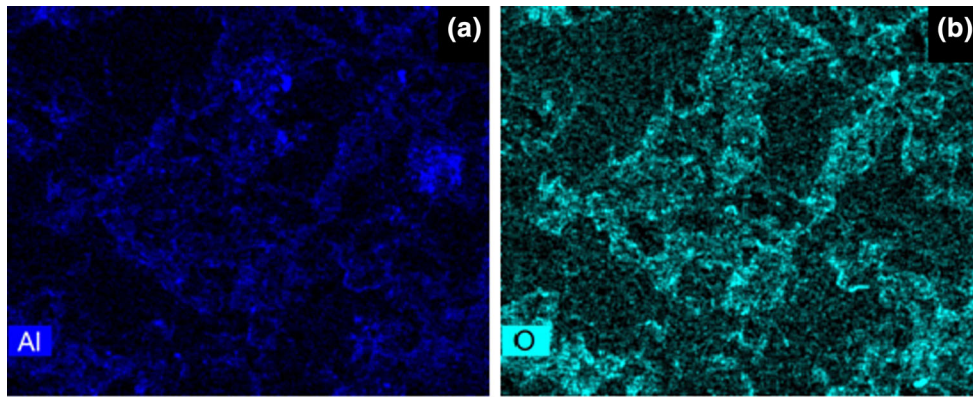
Fig. 2 Oxygen (O) (a) and aluminum (Al) (b) EDS maps on galvanized steel surface
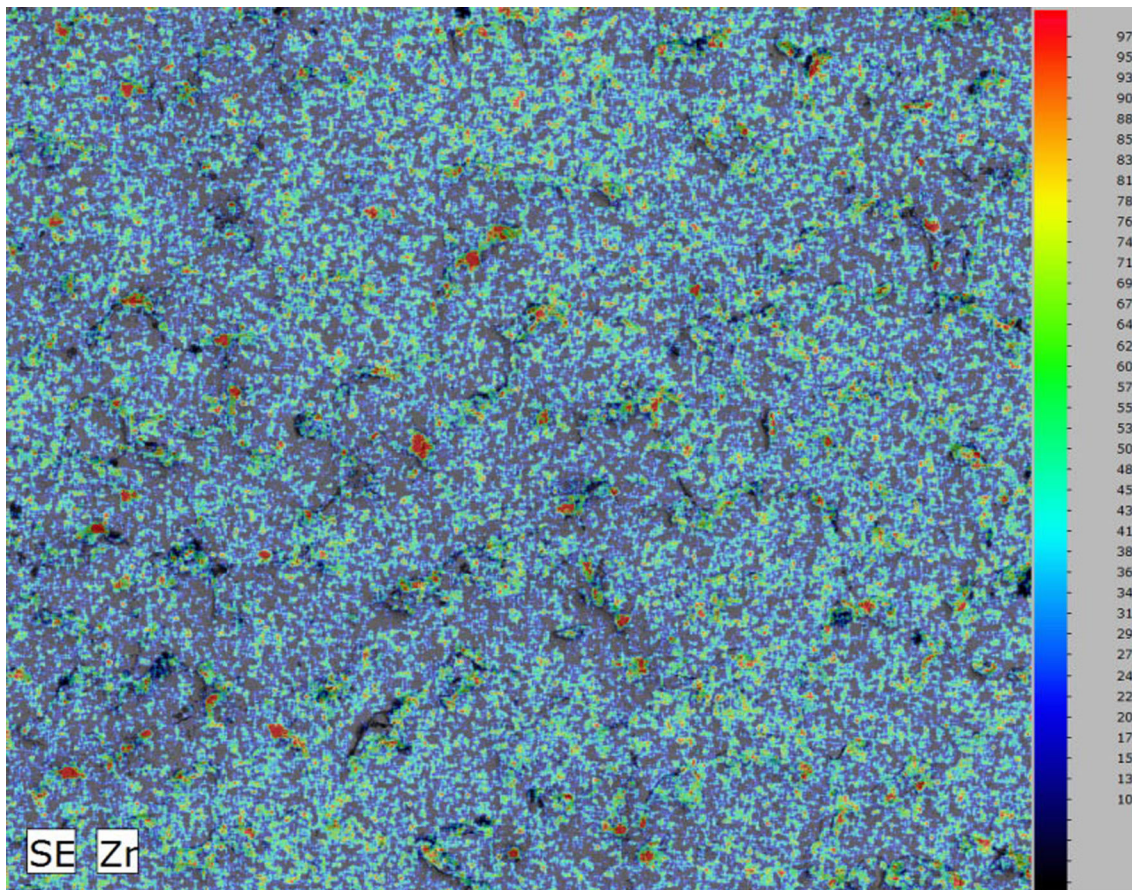
Fig. 3 Energy-dispersive spectroscopy (EDS) map of a secondary electron (SE) micrograph of zirconium (Zr)-based conversion coatings on galvanized steel

protective properties of phosphate and zirconium systems. This may be due to the development of pores in the organic coating.

According to the Bode diagram of Fig. 7(c), it is possible to notice that with the increase in the immersion time the phase angle for the two systems under study tends to decrease. Bode plot in Fig. 7(c) shows a phase angle close to $-60°$ for zirconium-treated samples, indicating a predominant resistive behavior. In contrast, the phosphate-treated system revealed phase angles close to $-80°$, which indicates a more capacitive behavior for a wide range of frequencies when compared with the zirconium system. The zirconium-treated samples have an impedance modulus of 10^5 Ω cm^2, two orders of magnitude smaller when compared to the initial measurements. Similarly, the phosphate-treated system showed a decrease in its impedance modulus; however, it was one order of magnitude higher than the impedance modulus of the zirconium system,

indicating a superior anti-corrosion performance of phosphate-treated systems at least for the first 120 days of immersion in an aqueous solution of NaCl.

EIS data were analyzed in terms of two equivalent circuits. Figure 8 shows the equivalent circuits fitted to the EIS data of the phosphate- and zirconium-treated samples after paint application: (Fig. 8a) 80 days and (Fig. 8b) 100 and 120 days of immersion in NaCl solution. The circuit consists of electrolyte resistance R_s, pore resistance R_{po}, coating capacitance C_c, double-layer capacitance C_{dl} and charge transfer resistance R_{ct}. The polarization resistance (R_p) is the sum of the pore resistance (R_{po}) and the charge transfer resistance (R_{ct}). Capacitance elements were modeled using a constant phase element (CPE) to also consider the electrochemical behavior of systems not corresponding exactly to a pure capacitance. Fitting was carried out using the Zview v 3.3 software (Scribner Associates).

The evolution of the fitted parameters is represented as a function of exposure time. Table 1 shows the evolution of the capacitance of the conversion coatings. The coating capacitance values (C_c) are associated with water uptake in the organic coating. Initially, the electrolyte penetrated through the coating and established conductive paths to the substrate, increasing the coating capacitance with exposure time. In general, painting schemes under service conditions present coating capacitance values between 10^{-11} and 10^{-9} F cm^{-2} (Ref 25). The coating capacitance (C_c) for the studied systems increased as the immersion time increased. Although a significant difference was not observed between the phosphate and zirconium treatment after 120 days of immersion, phosphated samples showed less C_c values (less water uptake ratio) compared to the zirconium-treated samples.

The double-layer capacitance (C_{dl}) is associated with the competition between paint delamination and the corrosion products accumulation at the interface (Ref 26). The evolution of C_{dl} with the immersion time (Table 1) exhibited a more pronounced increase for zirconium-treated samples in relation to the phosphate samples, and this can be due to a higher active metal region for the zirconium system. The result was confirmed by SEM analysis (Fig. 3); uncovered areas (active metal) were identified on the zirconia-treated galvanized steels, in contrast to phosphated galvanized samples which showed a homogeneous phosphate layer. The zirconium-treated sample revealed a value of C_{dl} equal to 1.6×10^{-5} F cm^{-2} during the first 100 days of immersion, while the phosphate system presented values of C_{dl} equivalent to 1×10^{-5} F cm^{-2} at the same time. After 120-day immersion, values of C_{dl} for zirconium and phosphate treatment reached values of 8×10^{-5} and 4.3×10^{-5} F cm^{-2}, respectively.

Charge transfer resistance (R_{ct}) is associated with the reactions at the coating–substrate interface. Phosphate-treated samples exhibited a R_{ct} equal to 3.9×10^5 Ω cm^2 after 120 days of immersion, unlike zirconium-treated samples that registered values of R_{ct} equal to 3×10^4 Ω cm^2 (Table 1). The decrease in the charge transfer resistance (Rct) with the exposure time may be due to increased corrosion rate or the presence of a greater active metallic area under the organic coating.

3.3 Porosity Evaluation

This porosity measurement expresses the number of open pores per coated area or the area of substrate exposed to the medium through the pores. Open pores induce the electrochemical corrosion by allowing the penetration of water and the diffusion of ionic impurities, compromising the anti-corrosion performance and other functional properties of the system. In general, a lower porosity means a smaller corrosion rate of substrate (Ref 14).
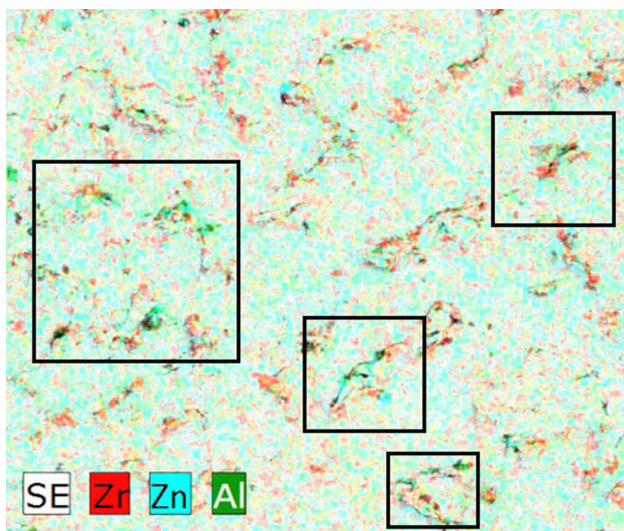
Fig. 4 Zirconium (Zr), zinc (Zn) and aluminum (Al) EDS maps on secondary electron (SE) image of zirconium-treated galvanized steel
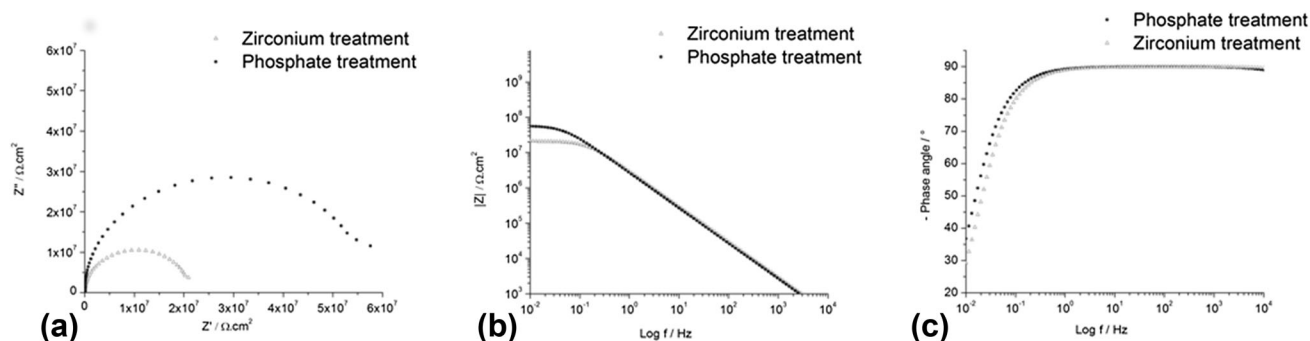
Fig. 5 Electrochemical impedance plots (a) Nyquist, (b) Bode diagram of impedance modulus vs. frequency and (c) Bode diagram of phase angle vs. frequency for phosphate-treated and zirconium-treated steel, after 80 days of immersion in NaCl solution
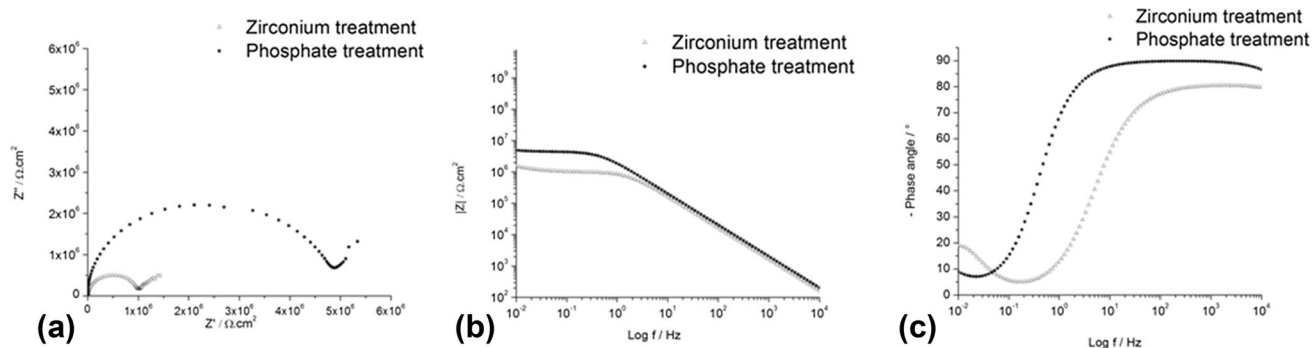
Fig. 6 Electrochemical impedance plots (a) Nyquist, (b) Bode diagram of impedance modulus vs. frequency and (c) Bode diagram of phase angle vs. frequency for phosphate-treated and zirconium-treated steel, after 100 days of immersion in NaCl solution
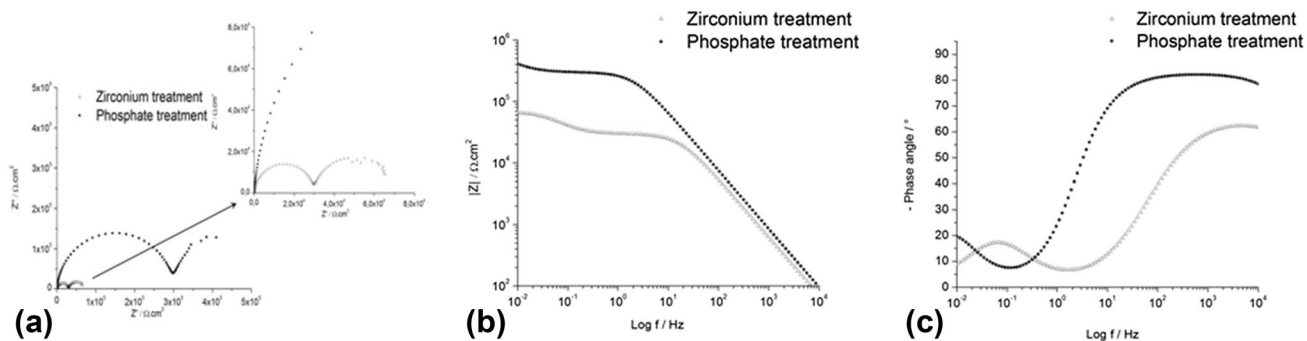
Fig. 7 Electrochemical impedance plots (a) Nyquist, (b) Bode diagram of impedance modulus vs. frequency and (c) Bode diagram of phase angle vs. frequency for phosphate-treated and zirconium-treated steel, after 120 days of immersion in NaCl solution

The polarization curve obtained using the Tafel analysis for bare galvanized steel sample is shown in Fig. 9. The electrochemical parameter obtained was the anodic Tafel coefficient: $\beta_a = 403.8 \times 10^{-3}$ V decade^{-1}.

The experimental EIS data showed two capacitive semicircles at high and low frequencies, respectively (Fig. 10). The first capacitive semicircle is related to the coating. The second semicircle is related to the corrosive process by charge transference.

The results obtained from the electrochemical impedance spectroscopy measurements for the bare galvanized steel, phosphate-treated steel and zirconium-coated steel are shown in Table 2. The equivalent circuit proposed for modeling the impedance response of all samples is shown in Fig. 8(b).

The porosity of the conversion coating was determined according to Eq 1. The polarization resistance of bare substrate (galvanized steel), R'_p, and the polarization resistance of coated substrate (phosphate and zirconium treatment), R_p, were obtained by using EIS technique (Table 2). The anodic Tafel coefficient of bare substrate was calculated by Tafel analysis.

The porosity found for the zirconium layer was $4 \pm 0.9\%$, in contrast to the phosphate layer that exhibited a porosity equivalent to $0.7 \pm 0.1\%$.

The porosity obtained for tricationic phosphate coating ($0.7 \pm 0.1\%$) agrees with the studies carried out by Ponte et al. (Ref 27). Teixeira et al. (Ref 28) also found similar porosity values for the tricationic phosphate layer processed by immer-

sion using a refiner on substrates of electrogalvanized ($1.4 \pm 0.1\%$) and hot-dip galvanized steels ($1.1 \pm 0.1\%$). The tricationic phosphate processed by spraying on hot-dip galvanized steels showed a porosity of $4.7 \pm 1.7\%$, similar to that found for the zirconium coating (Ref 28). The refiner and the process type play a key role on the porosity of the tricationic phosphate on electrogalvanized, hot-dip galvanized and galvannealed steels (Ref 28). For the phosphating by immersion without a refiner, the porosity of tricationic phosphate reached $16.8 \pm 6.4\%$ (Ref 28).

In terms of corrosion behavior, coated samples with a lower porosity present a higher corrosion resistance compared to coatings with a higher porosity (Ref 29). Teixeira et al. (Ref 29) reported that the porosity control of phosphated and painted steels is relevant to improve the corrosion resistance of these products used in automotive and home appliance industries. However, considering the adhesion performance, the porosity and surface roughness of the intermediate coating can promote the adhesion between substrate and a top layer.

The porosity obtained for zirconium coating ($4 \pm 0.9\%$) was higher than that reported in the literature (Ref 30). The high porosity of zirconium layer on galvanized steel can be explained due to the distribution and morphology of the defects present in the zinc coating as intermetallic sites enriched in aluminum, which favor the preferential nucleation of zirconium compounds. In the case of hot-dip galvanized steels, Saaremaa et al. (Ref 31) reported that the presence of Al_2O_3 on

the surface of the substrate reduces the reactivity and the uniformity of conversion pretreatment layer on the steel surface.

The porosity values agree with polarization resistance (R_p) and the coating capacitance data (C_c), shown in Fig. 9. Smaller values of R_p and higher values of C_c can be associated with a higher porosity coating. C_c can be considered proportional to active metal area (higher porosity), unlike R_p, which exhibits higher resistance values as the active area decreases (Ref 32).

3.4 Corrosion Resistance: Accelerated and Field Test

Accelerated corrosion test, according to the GM 14872 standard, and field test with a saline solution spray, according to the ISO 11474 standard, were performed on treated and painted steel samples. The corrosion resistance was measured in terms of the actual length of disbonded area in mm of the paint film starting from the scratch. The results of average scribe delamination on coated samples are presented in Table 3. Figures 11 and 12 show the images of treated and painted steel samples submitted to the GM 14872 cyclic accelerated corrosion test and the ISO 11474 accelerated field test, respectively. Table 3 and Fig. 11 and 12 show that the accelerated field test is less aggressive to the coated steel samples than the cyclic accelerated corrosion test. After 1 year of accelerated field test, the average scribe delamination of the paint was slightly higher for the zirconium-treated samples (0.34 mm) than for phosphate-treated steels (0.25 mm). According to the results of GM 14872 accelerated corrosion

test (3840-h exposure) shown in Table 3, phosphate-treated samples showed an average scribe delamination length of 0.31 mm, while the zirconium-treated samples showed a delamination displacement of 0.49 mm. Considering treated and painted steel samples, the average scribe delamination results were higher for the GM 14872 test when compared with the field test with a saline solution spray. This is due to the lower aggressiveness of field tests with a saline spray. The reason for this result is given in methodology where the aggressive condition of GM test was detailed. Salt solutions (0.9% w/v NaCl, 0.1% w/v CaCl$_2$ and 0.075% w/v NaHCO$_3$) were sprayed directly on the test samples for 15 min. Samples remained in the wet chamber for 75 min at 25 ± 2 °C without salt spray. This procedure was repeated 4 times before the next step. During the accelerated field test, a saline solution was sprayed on the steel samples only twice a week.

The visual evaluation of the coated samples after the exposure period showed the presence of blistering along the cut edges, mainly for the zirconium-treated samples (Fig. 11b), leading to the loss of adhesion of the organic coating on the metal substrate. Red rusting was observed at cut edges in Fig. 11. The atmospheric corrosion mechanism of iron is reported in the literature (Ref 33). The primary reaction products formed on iron steel are hydrated Fe^{2+} ions which are further oxidized by oxygen to Fe^{3+} and then precipitated as oxides, hydroxides and oxyhydroxides (FeOOH) with a reddish color as observed in Fig. 11 (Ref 34). Water can penetrate the painting coating through pores in the organic film causing swelling and reaching the paint–metal interface. After disbond-
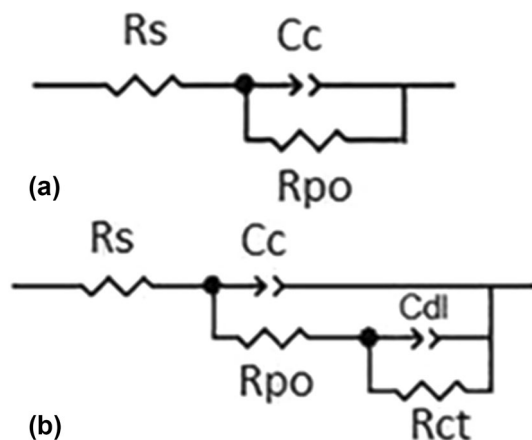
Fig. 8 Electrical equivalent circuits used to model the behavior of the treated and painted steel samples: (a) for 80 days and (b) for 100 and 120 days in NaCl solution
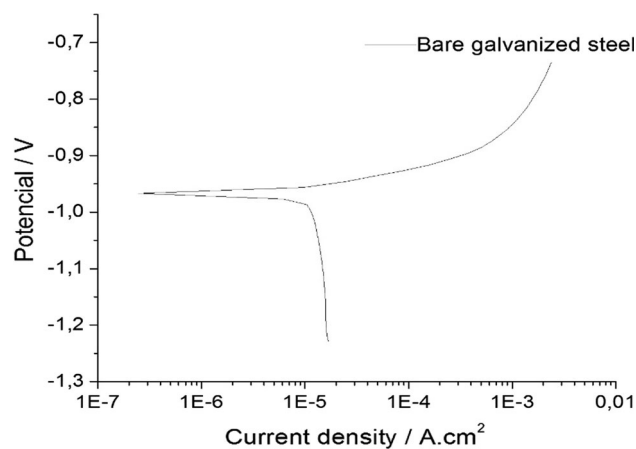
Fig. 9 Bare galvanized steel polarization curve, obtained using Tafel analysis in 3.5 wt.% NaCl solution

Table 1 Values of double-layer capacitance, coating capacitance and charge transfer resistance of phosphate- and zirconium-treated steels for 80, 100 and 120 days of immersion in a saline solution

Treatment	Immersion time, days	Double-layer capacitance, F cm^{-2} ($\times 10^{-5}$)	Coating capacitance, F cm^{-2} (10^{-8})	Charge transfer resistance, Ω cm^2 (10^4)
Phosphate	80	…	5	…
	100	1.0	3	670
	120	4.3	21	39
Zirconium	80	…	6	…
	100	1.6	10	160
	120	8.0	40	3
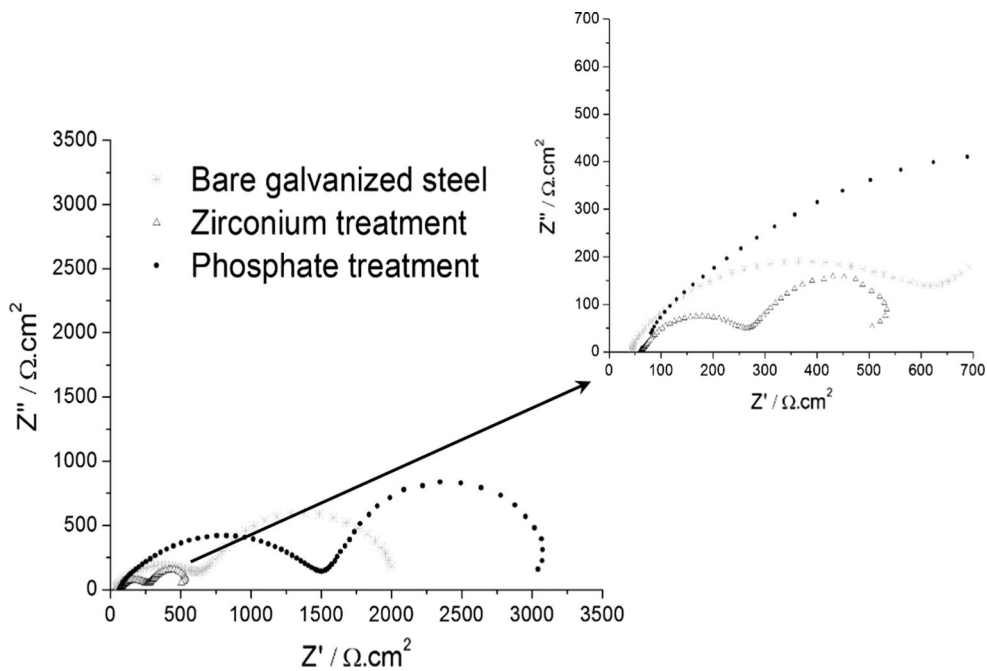
Fig. 10 Nyquist plots of bare galvanized steel (star), phosphate-treated steel (filled circle) and zirconium-treated steel (triangle)

Table 2   Electrochemical parameters obtained using the EIS technique

	Parameters	Bare galvanized steel	Phosphated steel	Zirconium-treated steel
E_{corr}, V	Corrosion potential	-1.017	-1.011	-1.010
C_c, F cm^{-2}	Coating capacitance	3.02×10^{-5}	4.88×10^{-6}	1.12×10^{-4}
C_{dl}, F cm^{-2}	Double-layer capacitance	0.0011	0.00083	0.0055
R_s, Ω cm^2	Solution resistance	39.2	46.82	61.23
R_{po}, Ω cm^2	Pore resistance	591.8	1505	224.4
R_{ct}, Ω cm^2	Charge transfer resistance	1619	1779	325.1
R_p, Ω cm^2	Polarization resistance	2210.8	3284	549.5

Table 3   Cyclic corrosion and natural exposure test results of painted coated steels

Substrate	Accelerated corrosion test (GM14872)3840 h	Field test with a saline solution spray (ISO11474)1 year
Phosphate-treated steel	0.31 ± 0.04	0.25 ± 0.03
Zirconium-treated steel	0.49 ± 0.08	0.34 ± 0.15

ing of the painting film, the non-uniform dissolution of carbon steel resulted in a non-uniform formation of γ-FeOOH and an amorphous ferric oxyhydroxide (Ref 20, 33, 34).

4. Conclusions

The zirconium EDS map showed a non-uniform and heterogeneous distribution of zirconium on the steel surface due to preferential nucleation of the zirconium on the aluminum-rich sites on the surface of galvanized steel.

According to the EIS results, the samples treated with zirconium showed charge transfer resistance comparable to the phosphate samples during the first 100 days of immersion in a saline solution. However, after 120 days of immersion, the charge transfer resistance was one magnitude order lower than the impedance of the phosphated samples.

According to the results of GM 14872 accelerated corrosion test (3840-h exposure) and the results of 1 year of exposure to the accelerated field test, phosphate-treated samples showed an average scribe delamination length lower than the zirconium-treated samples.

The accelerated field test was less aggressive to the phosphate-treated and zirconium-treated steel samples than the GM 14872 accelerated corrosion test.

The porosity found for the zirconium-treated sample was $4 \pm 0.9\%$, in contrast to the tricationic phosphate coating that exhibited a porosity equivalent to $0.7 \pm 0.1\%$. The higher
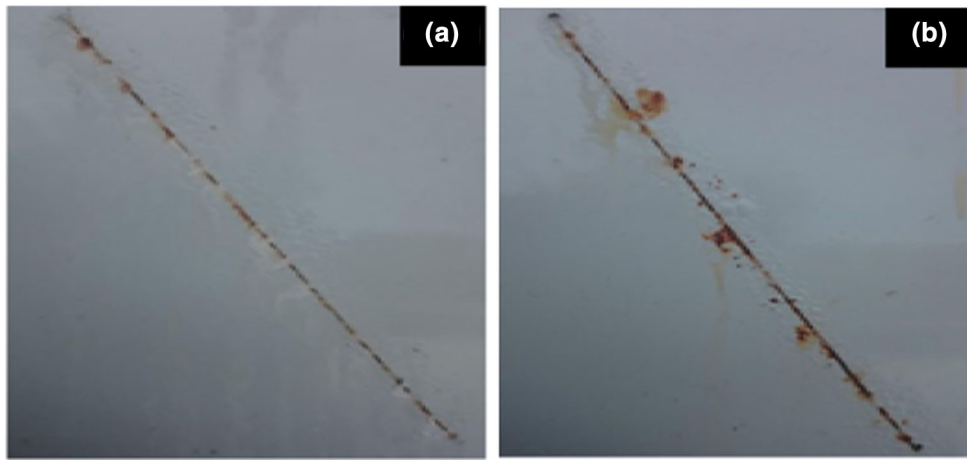
Fig. 11 Painted samples of phosphate treatment (a) and zirconium treatment (b) after 3840 h of GM 14872 cyclic accelerated corrosion test
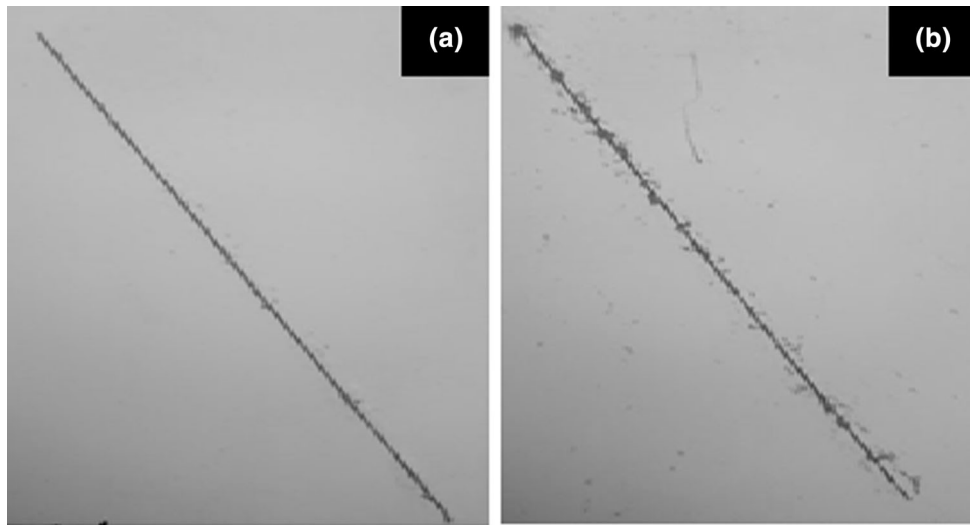
Fig. 12 Painted samples of phosphate treatment (a) and zirconium treatment (b) after 1 year of natural exposure field test accelerated with a saline solution spray according to the ISO 11474 Standard

porosity of the zirconium-treated coatings agrees with the lower corrosion resistance of the zirconium-treated samples.

References

1. V. Kuklik and J. Kudlacek, *Hot-dip Galvanizing of Steel Structures*, Butterworth-Heinemann, Boston, 2016
2. J.F. Van Eijnsbergen, *Duplex Systems: Hot-Dip Galvanizing Plus Painting*, Elsevier, Amsterdam, 1994
3. S. Adhikari, K.A. Unocic, Y. Zhai, G.S. Frankel, J. Zimmerman, and W. Fristad, Hexafluorozirconic Acid Based Surface Pretreatments: Characterization and Performance Assessment, *Electrochim. Acta*, 2011, **56**(4), p 1912–1924
4. A. Tiwari, L. Hihara, and J. Rawlins, Ed., *Intelligent Coatings for Corrosion Control*, Butterworth-Heinemann, Boston, 2015
5. T.S. Narayanan, Surface Pretreatment by Phosphate Conversion Coatings—A Review, *Rev. Adv. Mater. Sci.*, 2005, **9**(2), p 130–177
6. B. Tepe and B. Gunay, Evaluation of Pre-treatment Processes for HRS (Hot Rolled Steel) in Powder Coating, *Prog. Org. Coat.*, 2008, **62**(2), p 134–144
7. C. Klingenberg and D. Jones, Low-Temperature, Phosphate-Free Conversion Coatings: A Cost-Effective, High-Performance, Environmentally Friendly Alternative to Iron Phosphate, *Metal Finish.*, 2007, **105**(9), p 28–30
8. G. Gusmano, G. Montesperelli, M. Rapone, G. Padeletti, A. Cusmà, S. Kaciulis, A. Mezzi, and R. Di Maggio, Zirconia Primers for Corrosion Resistant Coatings, *Surf. Coat. Technol.*, 2007, **201**(12), p 5822–5828
9. S. Verdier, N. Van der Laak, F. Dalard, J. Metson, and S. Delalande, An Electrochemical and SEM Study of the Mechanism of Formation, Morphology, and Composition of Titanium or Zirconium Fluoride-Based Coatings, *Surf. Coat. Technol.*, 2006, **200**(9), p 2955–2964
10. A. Ghanbari and M.M. Attar, Corrosion Behavior of Zirconium Treated Mild Steel With and Without Organic Coating: A Comparative Study, *Surf. Rev. Lett.*, 2014, **21**(06), p 1450088

11. D. Weng, P. Jokiel, A. Uebleis, and H. Boehni, Corrosion and Protection Characteristics of Zinc and Manganese Phosphate Coatings, *Surf. Coat. Technol.*, 1997, **88**(1–3), p 147–156

12. J. Creus, H. Mazille, and H. Idrissi, Porosity Evaluation of Protective Coatings Onto Steel, Through Electrochemical Techniques, *Surf. Coat. Technol.*, 2000, **130**(2), p 224–232

13. L. Kwiatkowski, Phosphate Coatings Porosity: Review of New Approaches, *Surf. Eng.*, 2004, **20**(4), p 292–298

14. V.D.F.C. Lins, G.F. de Andrade Reis, C.R. de Araujo, and T. Matencio, Electrochemical Impedance Spectroscopy and Linear Polarization Applied to Evaluation of Porosity of Phosphate Conversion Coatings on Electrogalvanized Steels, *Appl. Surf. Sci.*, 2006, **253**(5), p 2875–2884

15. GM 14872, *General Motors Engineering Standards Materials and Processes Procedures Accelerated Corrosion Test—Method B* (2010)

16. ISO 11474, *Corrosion of Metals and Alloys: Corrosion Tests in Artificial Atmosphere—Accelerated Outdoor Test by Intermittent Spraying of Salt Solution* (1993)

17. ASTM D1654-08, *Standard Test Method for Evaluation Of Painted or Coated Specimens Subjected to Corrosive Environments*, ASTM International, West Conshohocken, 2008

18. S. Maeda, Surface Chemistry of Galvanized Steel Sheets Relevant to Adhesion Performance, *Prog. Org. Coat.*, 1996, **28**(4), p 227–238

19. R.M.V. Paranhos, V.F.C. Lins, A.A.M. Waldemar, and E.A. Alvarenga, Optimisation of Electrochemical Stripping of Galvannealed Interstitial Free Steels, *Surf. Eng.*, 2011, **27**, p 676–682

20. E.A. Alvarenga and V.F.C. Lins, Atmospheric Corrosion Evaluation of Electrogalvanized, Hot-Dip Galvanized, and Galvannealed Interstitial Free Steels Using Accelerated Field and Cyclic Tests, *Surf. Coat. Technol.*, 2016, **306**, p 428–438

21. F. Andreatta, A. Turco, I. De Graeve, H. Terryn, J.H.W. De Wit, and L. Fedrizzi, SKPFM and SEM Study of the Deposition Mechanism of Zr/Ti Based Pre-treatment on AA6016 Aluminum Alloy, *Surf. Coat. Technol.*, 2007, **201**(18), p 7668–7685

22. J. Cerezo, I. Vandendael, R. Posner, K. Lill, J.H.W. de Wit, J.M.C. Mol, and H. Terryn, Initiation and Growth of Modified Zr-Based Conversion Coatings on Multi-Metal Surfaces, *Surf. Coat. Technol.*, 2013, **236**, p 284–289

23. S. Feliu and M. Morcillo, The Reproducibility of Impedance Parameters Obtained for Painted Specimens, *Prog. Org. Coat.*, 1995, **25**(4), p 365–377

24. F. Deflorian and L. Fedrizzi, Adhesion Characterization of Protective Organic Coatings by Electrochemical Impedance Spectroscopy, *J. Adhes. Sci. Technol.*, 1999, **13**(5), p 629–645

25. B. Del Amo, L. Véleva, A.R. Di Sarli, and C.I. Elsner, Performance of Coated Steel Systems Exposed to Different Media: Part I. Painted Galvanized Steel, *Prog. Org. Coat.*, 2004, **50**(3), p 179–192

26. N. Tang, W.J. van Ooij, and G. Górecki, Comparative EIS Study of Pretreatment Performance in Coated Metals, *Prog. Org. Coat.*, 1997, **30**(4), p 255–263

27. H.D.A. Ponte, A.M. Maul, and E.D.A. Alvarenga, Analysis of Electrochemical Porosity of Phosphatized Coatings on Galvanized Steel Substrate, *Mater. Res.*, 2002, **5**(4), p 439–446

28. C.H.S.B. Teixeira, E.A. Alvarenga, W.L. Vasconcelos, and V.F.C. Lins, Effect of Porosity of Phosphate Coating on Corrosion Resistance of Galvanized and Phosphated Steels Part I: Measurement of Porosity of Phosphate, *Mater. Corros.*, 2011, **62**, p 771–777

29. C.H.S.B. Teixeira, E.A. Alvarenga, W.L. Vasconcelos, and V.F.C. Lins, Effect of Porosity of Phosphate Coating on Corrosion Resistance of Galvanized and Phosphated Steels Part II: Evaluation of Corrosion Resistance, *Mater. Corros.*, 2011, **62**, p 853–860

30. E. Ramanathan and S. Balasubramanian, Comparative Study on Polyester Epoxy Powder Coat and Amide Cured Epoxy Liquid Paint over Nano-Zirconia Treated Mild Steel, *Prog. Org. Coat.*, 2016, **93**, p 68–76

31. V. Saarimaa, A. Markkula, K. Arstila, J. Manni, and J. Juhanoja, Effect of Hot Dip Galvanized Steel Surface Chemistry and Morphology on Titanium Hexafluoride Pretreatment, *Adv. Mater. Phys. Chem.*, 2017, **7**(02), p 28

32. R.S. Razavi, *Recent Researches in Corrosion Evaluation and Protection*, InTech, Shanghai, 2012

33. E. McCafferty, *Introduction to Corrosion Science*, Springer, New York, 2010

34. M. Stratmann, K. Bohnenkamp, and H.J. Engell, An Electrochemical Study of Phase-Transitions in Rust Layers, *Corros. Sci.*, 1983, **23**, p 969–985